

SPIN EFFECTS IN LARGE RAPIDITY NEUTRAL PION PRODUCTION AT STAR

D.A. Morozov^{1†} for the STAR collaboration

(1) *Institute for High Energy Physics, Protvino, Russia*

† *E-mail: Dmitry.Morozov@ihep.ru*

Abstract

Measurements by the STAR collaboration of neutral pion production at large Feynman x (x_F) in the first polarized proton collisions at $\sqrt{s} = 200$ GeV were reported previously. During the following two runs additional statistics were acquired with an improved forward calorimeter for the π^0 cross-section and analyzing power measurements. First data from pp collisions at $\sqrt{s} = 410$ GeV were taken during the RHIC run that ended in June, 2005.

The cross section was measured at $\eta = 3.3, 3.8$ and 4.0 and was found to be consistent with next-to-leading order perturbative QCD calculations.

The analyzing power was found to be zero at negative x_F and at positive x_F up to 0.3 , then increased with increasing x_F . This behavior can be described by phenomenological models including the Sivers effect, the Collins effect or higher twist contributions in initial and final states.

Results for the analyzing power at $\eta = 3.7$ and 4.0 from all data acquired at $\sqrt{s} = 200$ GeV and the status of the analysis of the $\sqrt{s} = 410$ GeV data will be presented. Future upgrade plans and status will also be discussed.

Introduction

At present Quantum Chromodynamics (QCD) can not explain the origin of significant transverse single spin asymmetry (A_N) in partonic interactions. Collinear factorized perturbative QCD (pQCD) calculations at leading twist predict these analyzing powers to be entirely negligible, due to chirality in the theory. However, experimental data [1, 2, 3] shows that A_N for inclusive particle production is on the order of 10% independent of the center of mass energy (\sqrt{s}). To improve the situation theorists develop several models in a generalized version of the QCD factorization scheme, which allows for intrinsic transverse motion of partons inside hadrons, and of hadrons relatively to fragmenting partons. This adds new possibilities of spin effects, absent for collinear configurations. Sivers [4] proposed as a source of spin effects to be a flavor dependent correlation between the proton spin (\mathbf{S}_p), momentum (\mathbf{P}_p) and transverse momentum (\mathbf{k}^\perp) of the unpolarized partons inside the proton. This results in the new polarized parton distribution function:

$$f_{q/p^\uparrow}(x, \mathbf{k}_q^\perp; \mathbf{S}_p) = \hat{f}_{q/p}(x, k_q^\perp) + \frac{1}{2} \Delta^N f_{q/p^\uparrow}(x, k_q^\perp) \frac{\mathbf{S}_p \cdot (\mathbf{P}_p \times \mathbf{k}_q^\perp)}{|\mathbf{S}_p| |\mathbf{P}_p| |\mathbf{k}_q^\perp|}, \quad (1)$$

where $\hat{f}_{q/p}(x, k_q^\perp)$ - unpolarized distribution function, $\Delta^N f_{q/p^\uparrow}(x, k_q^\perp)$ - Sivers function and x is the Bjorken scaling variable. Also significant A_N could be produced by the

correlation between the quark spin (\mathbf{s}_q), momentum (\mathbf{p}_q) and transverse momentum (\mathbf{k}^\perp) of the pion in the final state. Such an approach has been introduced by Collins [5]. Then the fragmentation function of transversely polarized quark q takes the form:

$$D_{\pi/q^\uparrow}(z, \mathbf{k}_\pi^\perp; \mathbf{s}_q) = \hat{D}_{\pi/q}(z, k_\pi^\perp) + \frac{1}{2} \Delta^N D_{\pi/q^\uparrow}(z, k_\pi^\perp) \frac{\mathbf{s}_q \cdot (\mathbf{p}_q \times \mathbf{k}_\pi^\perp)}{|\mathbf{p}_q \times \mathbf{k}_\pi^\perp|}, \quad (2)$$

where $\hat{D}_{\pi/q}(z, k_\pi^\perp)$ - unpolarized fragmentation function, $\Delta^N D_{\pi/q^\uparrow}(z, k_\pi^\perp)$ - Collins function and z is longitudinal component of pion momentum. Along with Collins and Sivers mechanisms there are higher twist effects in either initial [6] or final [7] state which may cause the observed analyzing powers.

The Relativistic Heavy Ion Collider (RHIC) at Brookhaven National Lab (BNL) provides collisions of polarized protons at the energy of $\sqrt{s} = 200$ GeV since 2002. At 2005 first 410 GeV collisions of polarized protons have been detected. The Solenoidal Tracker at RHIC (STAR [8]) consists mainly of a large volume TPC, Forward TPC, Beam Beam Counters (BBC), Endcap Electromagnetic Calorimeter (EMC), Barrel Electromagnetic Calorimeter (BEMC) and Forward Pion Detector (FPD). This contribution will focus on results from FPD and BBC, which located in the very forward region of STAR coverage. BBC are segmented scintillator detectors surrounding the beam pipe. It provides the minimum bias trigger, absolute luminosity and relative luminosity for our experiment. In addition BBC coincidences are used to suppress beam gas background. FPD is a set of eight calorimeters of lead glass cells with size of 3.8 cm×3.8 cm×45 cm. It provides triggering and reconstruction of neutral pions. Four of them are left-right detectors and 7×7 arrays cells. Four others are top-bottom 5×5 arrays and are useful for systematics studies.

1 Single Spin Asymmetry at STAR/FPD

By definition single spin asymmetry is: $A_N = \frac{1}{P_{Beam}} \frac{d\sigma^\uparrow - d\sigma^\downarrow}{d\sigma^\uparrow + d\sigma^\downarrow}$, where P_{Beam} - polarization of transversely polarized beam, $d\sigma^{\uparrow(\downarrow)}$ - differential cross section of π^0 when incoming proton has spin up (down). One can measure A_N by two different ways. First with the use of single arm calorimeter: $A_N = \frac{1}{P_{Beam}} \frac{N^\uparrow - RN^\downarrow}{N^\uparrow + RN^\downarrow}$, where $N^{\uparrow(\downarrow)}$ - the number of pions detected when the polarization of the beam is oriented up(down) and $R = \frac{L^\uparrow}{L^\downarrow}$ is the spin dependent relative luminosity measured by BBC. Second with the use of two arms calorimeter ("cross-ratio" method): $A_N = \frac{1}{P_{Beam}} \frac{\sqrt{N_L^\uparrow N_R^\downarrow} - \sqrt{N_R^\uparrow N_L^\downarrow}}{\sqrt{N_L^\uparrow N_R^\uparrow} + \sqrt{N_R^\uparrow N_L^\downarrow}}$, where $N_{L(R)}^\uparrow$ - number of pions detected by the left (right) calorimeter while the beam has spin up and $N_{L(R)}^\downarrow$ - number of pions detected by the left (right) calorimeter while the beam has spin down. In this method one does not need the relative luminosity. The asymmetries from these two measurements were found to be consistent. Positive (negative) x_F is defined when the pion is observed with the same (opposite) longitudinal momentum as the polarized beam. Positive A_N is defined as more π^0 going left of the upward polarized beam. In the 2002 proton run 0.15 pb⁻¹ of integrated luminosity was collected for transversely polarized proton collisions at $\sqrt{s} = 200$ GeV at an average polarization of 16%. In 2003 run the integrated luminosity and average polarization have been increased to 0.5 pb⁻¹ and 27% respectively. In 2005(run 5) we collected 0.4 pb⁻¹ of $\sqrt{s} = 200$ GeV data with polarization

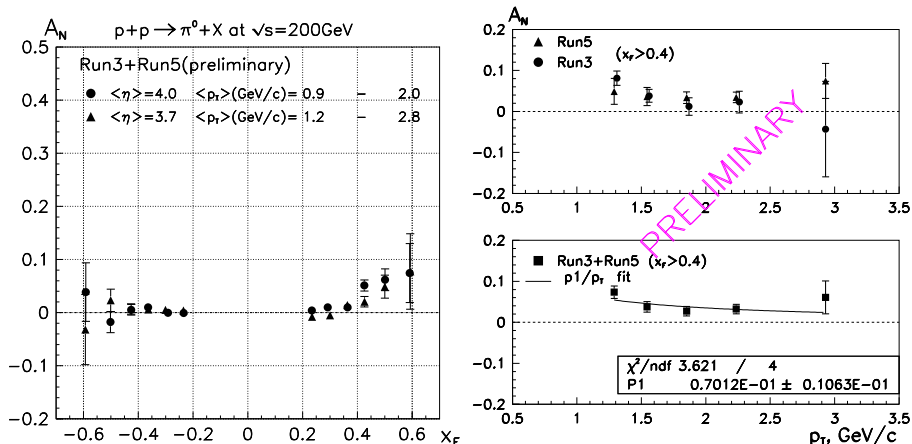


Figure 1: Left: Analyzing power of π^0 in $p^+p \rightarrow \pi^0 X$ reaction in run3 and run5 as a function of x_F . Right-top: Analyzing power in run3 and run5 as a function of p_T at $x_F > 0.4$. Right-bottom: Analyzing power as a function of p_T at $x_F > 0.4$, combined data from run3 and run5.

of 45%. The polarization was measured by pC CNIPolarimeter [10]. All mentioned values of polarization are based on the online results from CNI polarimeter.

Earlier result from published 2002 data for $\langle \eta \rangle = 3.8$ [11] consistent with measurements at lower $\sqrt{s} = 20$ GeV (E704 experiment) and increasing with x_F . It also can be described by all theoretical predictions mentioned above due to statistical uncertainties. Preliminary results from run 2003 at $\langle \eta \rangle = 4.1$ were reported earlier [12]. The analyzing power for positive x_F at $\langle \eta \rangle = 4.1$ is consistent with zero up to $x_F \sim 0.35$, then increases with increasing x_F . The first measurement of A_N at negative x_F has been done, and is found to be zero. Negative x_F results may give an upper limit on the gluon Sivers function [13]. Using the same analysis as in run3 we extracted analyzing power from run5. Preliminary results from run5 data are shown at the Fig. 1. Left plot represents $A_N(x_F)$ dependencies from run3 and run5 data. We combined data from two runs since the results are consistent. There are two sets of points on the plot - for $\langle \eta \rangle = 3.7$ and for $\langle \eta \rangle = 4.0$. These numbers reflect two different working positions of the calorimeters - closer and farther to the beam respectively. A_N is nonzero at $x_F > 0.4$ and zero for negative x_F . The work on systematic errors calculations and single arm results (for consistency check with "cross-ratio" method) is in progress. On the right plot of Fig. 1 one can see p_T dependence of analyzing power for $x_F > 0.4$. Top plot shows $A_N(p_T)$ for run3 and run5 data separately. In the bottom plot we combined data from two runs. There is an evidence that analyzing power at $x_F > 0.4$ decreases with increasing p_T . To interpret and compare these data with theory we need to add systematic errors and single arm data.

2 Differential cross sections for forward π^0 -Production

The inclusive differential cross section for π^0 production for $30 < E_\pi < 55$ GeV at $\langle \eta \rangle = 3.8$ was previously published [11]. The result at $\langle \eta \rangle = 3.3$ in 2002 run also

have been extracted. In 2003 run new calorimeters and readout electronics have been installed to allow measurements of the differential cross section at $\langle \eta \rangle = 4.0$. The results are shown in Fig. 2.

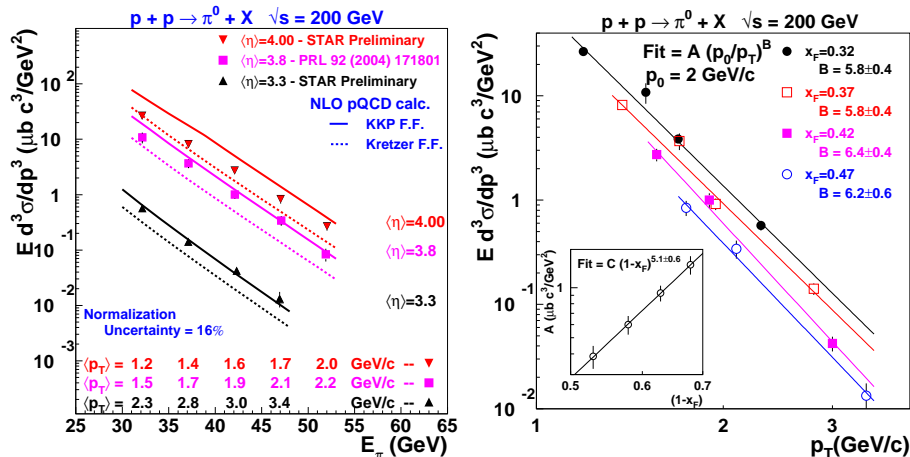


Figure 2: Left: invariant cross section for π^0 produced in pp collisions at $\sqrt{s} = 200$ GeV versus pion energy (E_π) at average pseudorapidities ($\langle \eta \rangle$) 3.3, 3.8 and 4.0. The error bars are point-to-point systematic and statistical errors added in quadrature. Right: invariant cross section as a function of p_T at fixed x_F (outer) and as a function of $(1 - x_F)$ at fixed $p_T = 2$ GeV/c (inner). Lines are fits by the functions showed in the plot.

On the left plot the cross sections are shown versus pion energy and are compared with NLO pQCD calculations evaluated at $\eta = 3.3, 3.8$ and 4.0 . Two sets of fragmentation functions are used. The model calculations are consistent with the data in contrast to the data at lower \sqrt{s} (NLO pQCD calculations at $\sqrt{s} = 20$ GeV underpredict measured cross sections [14]). As η increases, systematics regarding the comparison with NLO pQCD calculations begin to emerge. The data at low p_T are more consistent with the Kretzer set of fragmentation functions. Similar trend was observed at mid-rapidity [15]. On the right plot the data is represented as in earlier experiments [16]. The outer picture shows cross section as a function of p_T at fixed x_F . The inner one – cross section as a function of $(1 - x_F)$ at fixed $p_T = 2$ GeV/c. Invariant cross section falls with p_T at fixed x_F with exponent (value ~ 6) independently on x_F . Data also show exponential dependence on x_F with fixed $p_T = 2$ GeV/c. The value of the fitted exponent (~ 5) may be sensitive to the interplay between hard and soft scattering processes. One note should be stated regarding systematics of this separated x_F and p_T dependencies. Data were accumulated in different conditions in different running years: with different calorimeters, with different readout electronics, taken in different kinematical regions.

3 Plans for the near-term future

From the run5 data at $\sqrt{s} = 410$ GeV we can extract unpolarized differential cross section as we did for $\sqrt{s} = 200$ GeV. It will allow us to separate $x_T = \frac{2p_T}{\sqrt{s}}$ and p_T dependence of

cross section: $E \frac{d^3\sigma}{dp^2} \propto \left(\frac{\sqrt{s}}{2p_T}\right)^A \left(\frac{1}{p_T}\right)^B (1-x_F)^N$, where $N \approx 5$ and $A+B \approx 6$ (see Fig.2 right).

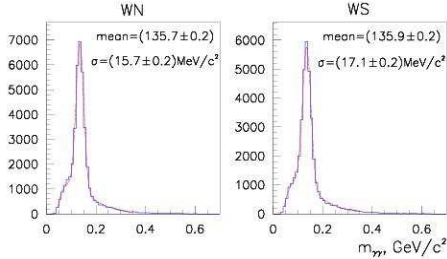


Figure 3: Di-photon invariant mass distributions for WS and WN modules of FPD from run5 at $\sqrt{s} = 410$ GeV.

FPD++ detectors will cover a broader range of $\Delta\eta$ and $\Delta\phi$.

We have recently proposed to assemble a Forward Meson Spectrometer (FMS) [17]. The FMS will cover the range $2.5 < \eta < 4.0$ and give STAR nearly hermetic electromagnetic coverage in the range $-1 < \eta < 4$. With the addition of the FMS, which has more than 25 times larger area coverage than the FPD, we will be able to achieve at least three physics objectives: a measurement of the gluon density distributions in gold nuclei for $0.001 < x < 0.1$; characterization of correlated pion cross sections as a function of p_T to search for the onset of gluon saturation effects associated with macroscopic gluon fields; measurements with transversely polarized protons that are expected to resolve the origin of the large transverse spin asymmetries in $p_{\uparrow} + p \rightarrow \pi^0 + X$ reactions for forward π^0 production. The expected completion of FMS is by October 2006.

Summary

Large spin effects have been observed at forward π^0 production in polarized pp collisions at energy $\sqrt{s} = 200$ GeV at STAR FPD. The single spin asymmetry for positive x_F is consistent with zero up to $x_F = 0.35$, then increases with increasing x_F . The asymmetry is found to be zero for negative x_F . First result for the $A_N(p_T)$ was obtained using combined statistics from run3 and run5. There is an evidence that the π^0 analyzing power at $x_F > 0.4$ decreases with increasing p_T . The inclusive differential cross section for forward π^0 production at $\sqrt{s} = 200$ GeV is consistent with NLO pQCD calculations in contrast to what was observed at lower energy. First try to map the cross section in $x_F - p_T$ plane was performed. The near-future plans are planning enhancement of

This work is in progress. As an example of reconstruction of π^0 mesons at $\sqrt{s} = 410$ GeV, the invariant mass distributions for two different FPD modules are shown at Fig. 3. The resolution in di-photon invariant mass distribution is better than 20 MeV. Existing FPD detectors well suited to large rapidity inclusive π^0 reconstruction. The next step will be an implementation of interim forward calorimeter FPD++ for RHIC run6 designed for single γ detection (schematic view is shown at Fig. 4). FPD++ will substitute west side of FPD detector. By design it represents as two Lead glass counter matrices. Each consists of 14×14 of 5.8×5.8 cm² cells with a space 4×4 in the middle for 6×6 smaller cells (3.8×3.8 cm²).

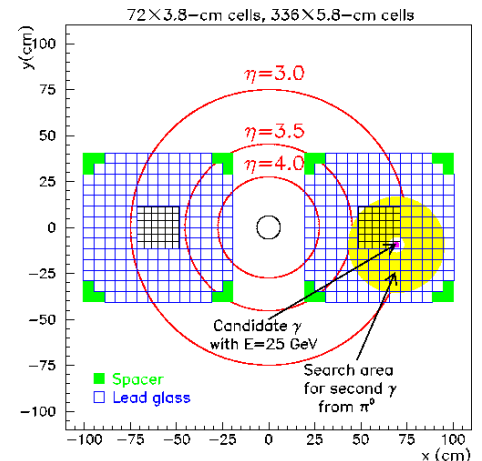


Figure 4: The FPD++ layout with isolation cut for single photon events. Circles represent different values of $\eta = 3.0, 3.5, 4.0$.

forward calorimeter for RHIC run6 FPD++ for γ/π^0 separation. The longer term future is upgrade in forward calorimetry in STAR (FMS) to probe low-x gluon densities and establish dynamical origin of A_N (complete upgrade by October 2006).

References

- [1] D.L. Adams *et al.*, *Phys. Lett. B* **261**, 201 (1991).
- [2] A.N. Vasiliev *et al.*, *Physics of Atomic Nuclei* **67**, 1495 (2004) Vol. 8.
- [3] K. Krueger *et al.*, *Phys. Lett. B* **459**, 412 (1999).
- [4] D.W. Sivers, *Phys. Rev. D* **41**, 83 (1990).
- [5] J.C. Collins *et al.*, *Nucl. Phys. B* **396**, 161 (1993).
- [6] J. Qui and G. Sterman, *Phys. Rev. D* **59**, 014004 (1998).
- [7] Y. Koike, AIP Conf. Proc. **675**, 449 (2003).
- [8] K.H. Ackermann *et al.*, *Nucl. Instrum. Methods A* **499**, 624 (2003).
- [9] J. Kiryluk, AIP Conf. Proc. **675**, 424 (2003).
- [10] O. Jinnouchi *et al.*, AIP Conf. Proc. **675**, 817 (2003).
- [11] J. Adams *et al.*, *Phys. Rev. Lett.* **92**, 171801 (2004).
- [12] A. Ogawa for the STAR collaboration, hep-ex/0412035, contribution to the SPIN2004 proceedings.
- [13] M. Anselmino *et al.*, *Phys. Rev. D* **71**, 014002 (2005).
- [14] C. Bourrely and J. Soffer, *Eur. Phys. J.C* **36**, 371 (2004).
- [15] S.S. Adler *et al.*, *Phys. Rev. Lett.* **91**, 241803 (2003).
- [16] J. Singh *et al.*, *Nucl. Phys. B* **140**, 189 (1978).
- [17] L.C. Bland *et al.*, *Eur. Phys. J. C* **43**, 427 (2005).